Materials Science-Poland, *Vol. 28*, *No. 1*, *2010*

Effect of thermal ageing on the evolution of microstructure and degradation of hardness of 2.25Cr-1Mo steel

B.B. JHA[1*], B.K. MISHRA[1], B. SATPATI[2], S.N. OJHA[3]

[1]Advanced Materials Technology Division, IMMT, Bhubaneswar-751013, India

[2]Materials Characterization Division, IMMT, Bhubaneswar-751013, India

[3]Department of Metallurgical Engineering, IT- BHU, Varanasi-221005, India

Thermal ageing of various durations and at various temperatures was performed in order to understand microstructural changes associated with precipitation and coarsening of carbides in 2.25Cr-1Mo steel. The severity of thermal ageing is expressed in terms of the Larson–Miller parameter (LMP). The microstructural examinations were carried out by optical and scanning electron microscopy techniques. A transmission electron microscope (TEM) and an electron probe micro analyzer (EPMA) were used to identify the carbide particles, and to analyse the shape, size and distribution of the precipitate phases. Influence of these precipitates on hardness degradation of the steel has been examined. The reasons for the variation in the microstructure and for the hardness degradation of steel arising from thermal ageing are discussed.

Keywords: *thermal ageing; microstructure; hardness degradation; 2.25Cr-1Mo steel*

1. Introduction

Ferritic 2.25Cr-1Mo steel is a popular engineering alloy used for high temperature applications such as heat exchangers, steam receivers, high temperature headers and piping in various power generating units [1]. As the service temperatures have been increasing to improve the thermal efficiency of power generating systems, materials having strong stability of microstructures and increased corrosion resistance at operating temperatures are needed for such applications. The main advantage of the steel under consideration is an improved high-temperature strength derived from molybdenum and chromium additions and the enhanced corrosion resistance derived from

*Corresponding author, e-mail: bbjha@immt.res.in

chromium [2]. The high temperature strength of this steel is derived mainly from two sources: solid solution strengthening of the ferrite matrix by carbon, molybdenum and chromium and precipitation hardening by carbides [3]. Due to its properties at elevated temperatures, this steel satisfies the safety criteria for operational use, as specified under section 3-ASME Case-47 of Ref. [4].

2.25Cr-1Mo ferritic steel has always been used in the normalized and tempered conditions or annealed conditions, depending upon the thickness of the component. Thin boiler tubes are made from steel in the annealed condition, whereas thick piping and headers are used mostly in the normalized and tempered conditions. Depending on cooling rates employed in these treatments, the microstructures of 2.25Cr-1Mo steel may vary from ferrite–pearlite aggregates to ferrite-bainite aggregates. The carbides obtained during the heat treatments are of the required morphology and distribution, so that the steel can maintain its strength at high temperature. However, due to the metastable nature of these precipitates, they undergo an undesirable transformation under operating conditions or during repair welding. Occasionally thermal transients can cause excessive local heating of the tubes, resulting in microstructural alteration [2, 5]. All these situations would result in microstructural variation of components quite different from the initial, optimized microstructure obtained in the normalized and tempered conditions, or after annealing.

2.25Cr-1Mo ferritic steel consists of bainite and ferrite containing iron carbides and fine M_2C type carbides in annealed condition. As the duration of ageing increases, a variety of secondary carbides like M_7C_3, $M_{23}C_6$ and M_6C gets precipitated [6, 7]. The precipitates also get coarsened with ageing. Such an evolution of precipitates, and their coarsening, influences the performance of this material at high temperatures. Although the microstructural instability of the steel, in terms of its cavity formation and its linkage under stress (leading to microcrack generation), is well documented [8, 9], but no systematic data is available on the microstructural deterioration due to carbide precipitation and coarsening. For this reason an investigation was made into microstructural degradation at various temperatures, together with subsequent analysis into how this influences hardness. Determination of the true state of degradation is an important consideration in the accurate assessment of the remaining operational lifetime of components.

2. Experimental

Materials. 2.25Cr-1Mo ferritic steel having nominal chemical composition (wt. %) C – 0.07, Mn – 0.42, Si – 0.019, S – 0.025, Cr – 2.28, P – 0.02, Mo – 0.98, Ni – 0.09, Fe – balance, has been used in the present investigation.

*Thermal ageing.*The starting material used in this study was shaped in the form of a plate 12 mm thick. From this plate strips measuring 12 ×12 × 250 mm^3 were cut using a power hacksaw and then machined to a size of 10 × 10 × 80 mm^3: the rolling directions were parallel to the length of the strips. These strips were then sealed in

evacuated quartz tubes and subject to annealing at 1223 K for 2 h. The temperature of the furnace was maintained constant, within an accuracy of ±1.0 K.

In order to study the microstructural degradation, these annealed strips were subject to ageing treatments at 873 K for 10 h, 923 K for 20 h, 973 K for 40 h and 973 K for 80 h using a tubular furnace. These treatments correspond to the values of the Larson–Miller parameter (LMP) of 33 012, 35 402, 37 846 and 38 374, respectively. Scales of the heat treated samples were then removed by coarse polishing on silicon carbide papers.

Metallography. Cubes of 10 × 10 × 50 mm^3 were cut from the heat treated samples, annealed and thermally aged to various degrees. These specimens were suitably mounted in a cold setting resin and were ground using successive grades of silicon carbide papers and then polished mechanically using 0.25 μ diamond paste for final, scratch-free polishing. Chemical etching was then done using a solution of 2 cm^3 HNO_3 in 100 cm^3 of methanol (i.e., 2% Nital) maximum for 10 s.

Chemically etched and dried specimens were examined under a Nikon make, metallurgical microscope (Model LV-150). Complete scanning was done at the lower magnification in order to extract the most representative microstructural features, which were then captured at higher magnification and presented as observations.

Scanning electron microscopy (SEM) and electron probe micro analysis (EPMA). All the heat treated samples, after chemical etching, were examined using a SEM (Joel Model-804 and a Hitachi Model S-3400 N) for phase identification. Energy dispersive X-ray Analysis (EDX) together with SEM was used for determination of the surface composition. An electron probe micro analyzer (Joel Model JXA-8100) was used to obtain the line scan profile showing the compositional variation of various elements in the matrix. X-ray images showing the elemental distribution of various elements in different phases was also obtained using EPMA. These analyses enabled identifying the concentration of solute atoms within the grains and at the grain boundaries: the state of deterioration of a given microstructure, namely the result of a particular ageing treatment, corresponded to a specific LMP value.

Transmission electron microscopy (TEM). For the transmission electron microscopy (TEM), very thin specimens ca. 0.5 mm thick were cut from various heat treated samples by electric discharge machining (EDM). These specimens were further thinned, using fine grade silicon carbide papers, up to a thickness of about 0.2 mm and then discs 3 mm in diameters were cut. They were further thinned by polishing both sides using silicon carbide papers and emery papers, up to the thickness of about 80 μ. The thickness of the discs was further reduced at the central portion, using a dimpler (M/s Gattan make), to a thickness of about 30 μ. Dimpled discs were then subject to ion milling till a fine perforated hole was made at the centre of the disc, enabling the adjacent area of the hole to be electron transparent.

A FEI make (model Tecnai G^2 20 twin) analytical transmission electron microscope operating at an accelerated voltage of 200 kV was used to identify carbides pre-

cipitated as a result of various degrees of ageing. Using this microscope it was possible to resolve the precipitates of size down to Angstrom level. Selected area diffraction (SAD) patterns from matrix containing precipitates, and also from precipitates alone, were obtained to ascertain the orientation difference of various carbide precipitates with that of the matrix. Microchemical analyses of precipitates were carried out using an EDX facility attached with TEM. The EDX attachment had a super ultra thin window with Si (Li) detector for analyzing the constituents. A combination of bright field and dark field imaging was carried out to ascertain a detailed morphology of the precipitates and their coarsening with respect to the increase in the degree of ageing.

Hardness measurement. Microhardness measurement of annealed (1223 K, 2 h) and aged specimens subject to various degrees of ageing, corresponding to LMP values of 33 012, 35 402, 37 846 and 38 374 was carried out using a microhardness tester (model RZD-00 of Leitz make). Indentations in both the phases were made with a diamond indenter using 0.5 N force and after measuring both the diagonals of the indentations, hardness values in VHN were obtained. Minimum of about five data points were taken for each measurement and the reported hardness values (Hv) in Table 1 are the average values of these five points. The maximum variation in the scatter of data was about 7.0%. This variation has also been indicated as an interval of confidence while plotting these hardness values in function of the L–M parameters.

3. Results and discussion

3.1. Microstructural analysis

Figure 1a shows the optical micrograph of 2.25Cr-1Mo steel in annealed conditions and Fig. 1b shows the same observed under SEM. The average initial grain size was measured and found to be 35 μm. Transmission electron micrographs of this sample showed fine precipitation of lenticular shaped carbides uniformly distributed within the grains of the bainitic matrix.

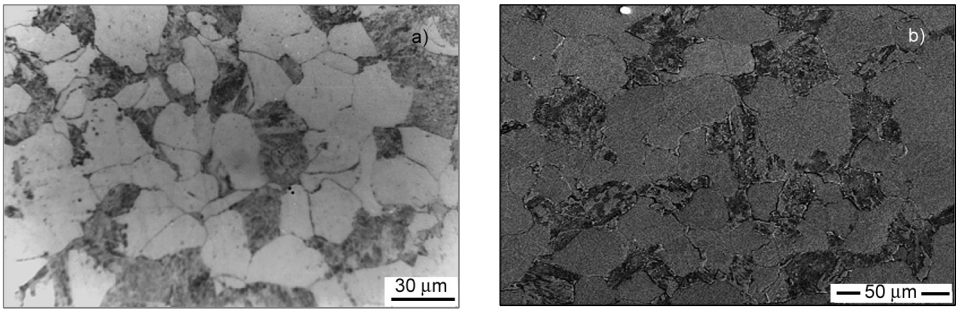

Fig. 1. Optical (a) and SEM (b) micrographs of 2.25Cr-1Mo steel showing bainite and ferrite phases after annealing (1223 K, 2h)

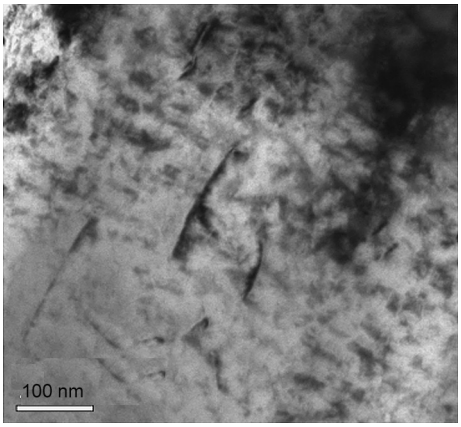

Fig. 2. Transmission electron micrograph of annealed 2.25Cr-1Mo steel showing lenticular precipitates of M_3C type in a bainite matrix

The shape of carbides is mostly lenticular, aligned parallel to each other along their axes, as shown in Fig. 2. It is observed that the size of these precipitates is of the order of about 100 nm. Figures 3a, b show the SAD pattern of a bainitic matrix containing these precipitates and their schematic indexing, respectively. The EDX results of 10–15 carbides showed them to be rich in iron. An EDX spectrum from typical carbide is shown in Fig. 4, which clearly revealed that these lenticular shaped carbides are of M_3C type, as observed by other workers [7, 10].

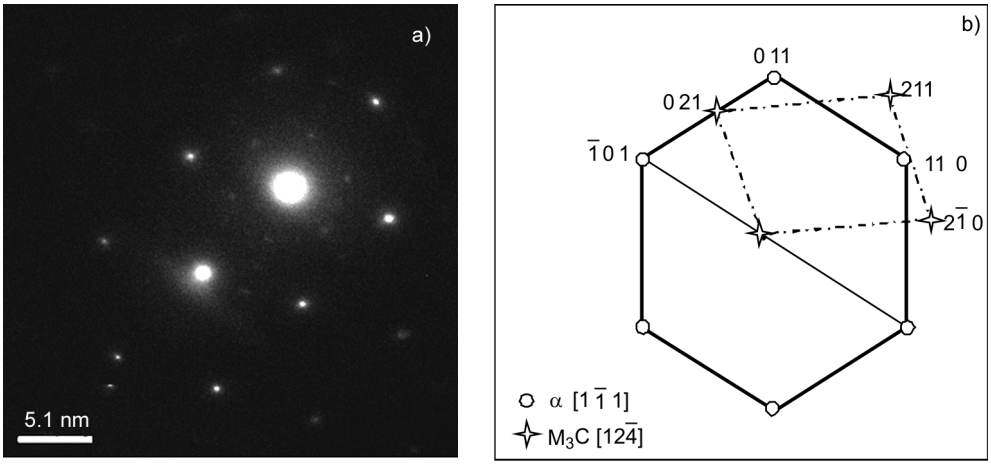

Fig. 3. SAD pattern of the bainitic matrix (a) containing precipitates of M_3C type in annealed 2.25Cr-1Mo steel and schematic indexing of a SAD pattern (b) shown in Fig. 3a

Transmission electron micrographs of the samples corresponding to the treatment of 873 K for 10 h (LMP = 33 012) showed the evolution of the needle type of precipitates, as shown in Fig. 5. The EDX results showed them to be rich in chromium with considerable iron contents. An EDX spectrum from typical carbide is shown in Fig. 6.

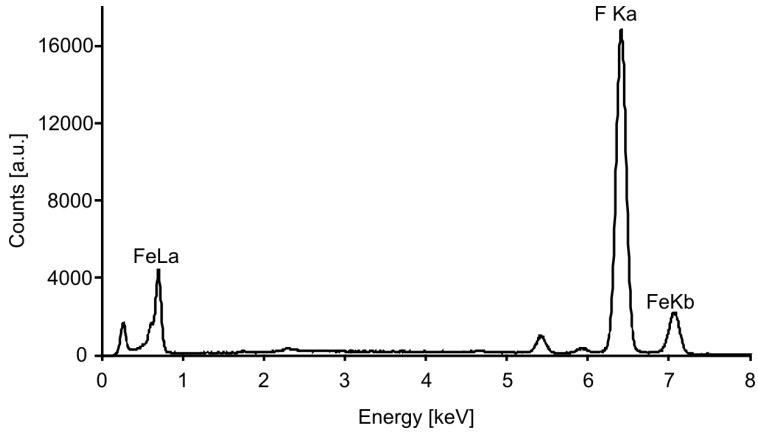

Fig. 4. Typical EDX spectrum of lenticular shaped iron rich carbide (M_3C type)

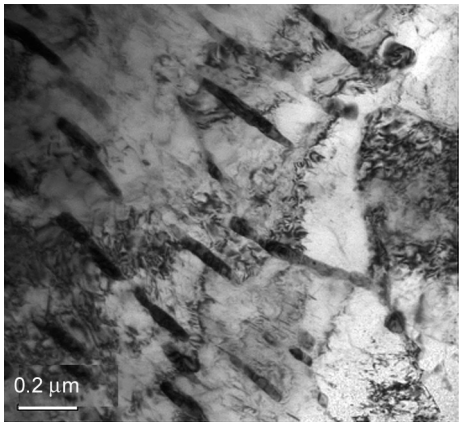

Fig. 5. Transmission electron micrograph of thermally aged 2.25Cr-1Mo steel (LMP = 33 012) showing precipitation of needle shaped carbides of a M_7C_3 type in a bainite matrix

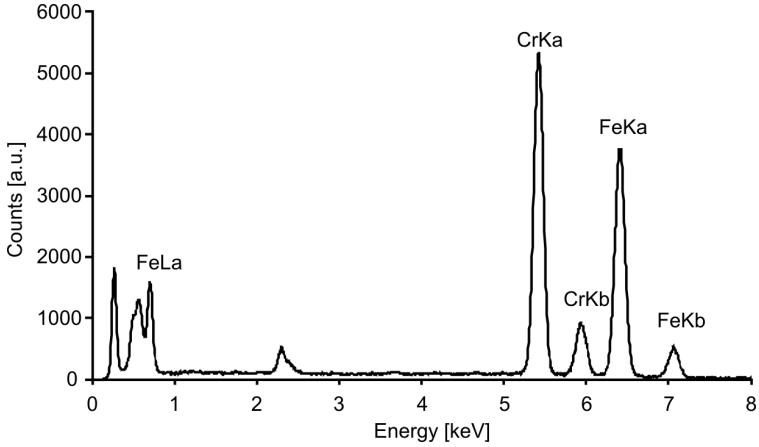

Fig. 6. Typical EDX spectrum of needle shaped carbide rich in chromium with considerable iron content (M_7C_3 type)

Selected area diffraction pattern, along with indexing of this kind of precipitates, showed a streaking pattern (Fig. 7) which is a typical characteristic of the M_7C_3 type of precipitates. These precipitates ca. 300 nm in size are also found to be oriented in the same direction.

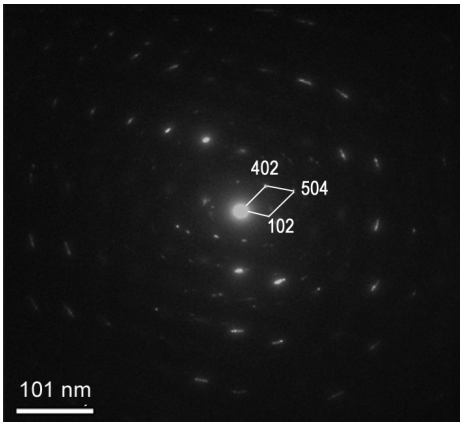

Fig. 7. SAD pattern of bainitic matrix containing precipitates of a M_7C_3 type showing streaking pattern along with indexing in thermally aged 2.25Cr-1Mo steel (LMP = 33 012)

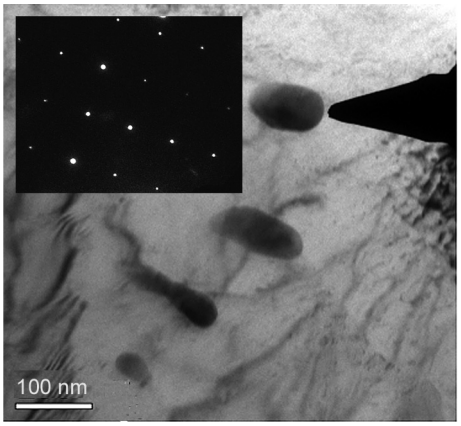

Fig. 8. Transmission electron micrograph of thermally aged 2.25Cr-1Mo steel (LMP = 35 402) showing precipitation of globular carbides of $M_{23}C_6$ type within the bainitic grain. The inset displays [100] zone of this phase

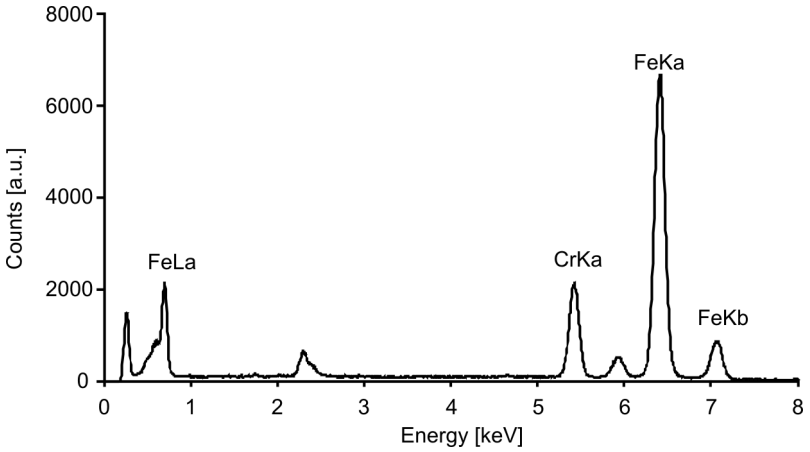

Fig. 9. Typical EDX spectrum of globular shaped carbide rich in iron with a considerable chromium content ($M_{23}C_6$ type)

Transmission electron micrographs of the samples corresponding to the treatment of 923 K for 20 h (LMP = 35 402) showed precipitation of globular carbides (size ca. 500 nm) within the bainitic matrix (Fig. 8). The inset of Fig. 8 also shows the SAD pattern from the precipitates along the zone axis [100]. The EDX results of these

globular shaped carbides showed them to be rich in iron with considerable chromium content. An EDX spectrum from typical globular shaped carbide is shown in Fig. 9. The spectrum revealed that these carbides are of $M_{23}C_6$ type, being at this stage rich in iron with a considerable chromium content. These observations suggest that globular precipitates evolved in bainitc matrix are different from those observed after the treatment at 873 K for 10 h (LMP = 33 012). The presence of $M_{23}C_6$ has also been reported by other workers [10] for this variety of steel and under this condition.

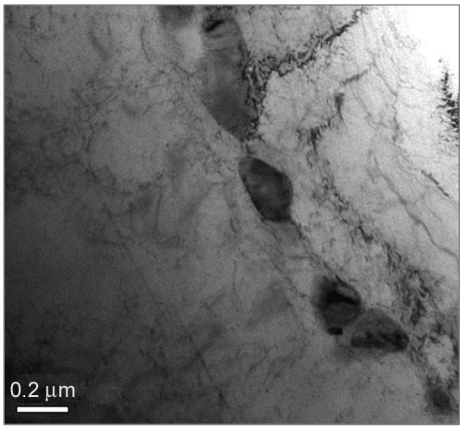

Fig. 10. Transmission electron micrograph showing precipitation of globular carbides of $M_{23}C_6$ type of at grain boundary in thermally aged 2.25Cr-1Mo steel (LMP = 37 846)

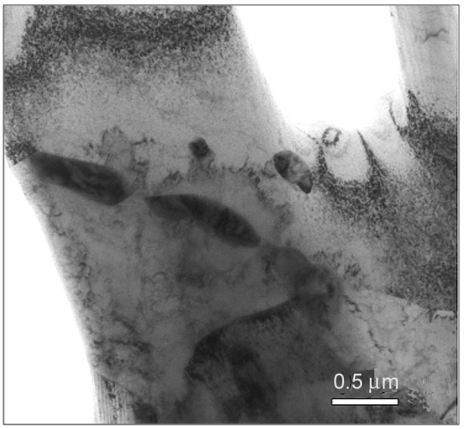

Fig. 11. Transmission electron micrograph showing precipitation of plate shaped carbides of M_6C type of at grain boundary in thermally aged 2.25Cr-1Mo steel (LMP = 37 846)

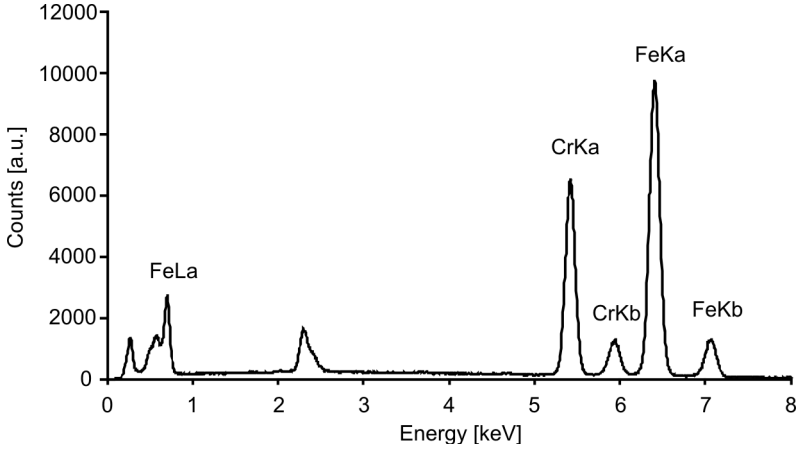

Fig. 12. Typical EDX spectrum of globular carbides rich in iron and chromium ($M_{23}C_6$ type)

Transmission electron micrographs of the specimen corresponding to the treatment at 973 K for 40 h (LMP = 37 846) are shown in Figs. 10 and 11. It is observed that by this treatment (LMP value of 37 846), the globular carbides have coarsened

and they are aligned at the grain boundaries. Their size has also increased (ca. 1 μ). Some plate shaped precipitates have also been observed (Fig. 11) as a result of this treatment. An EDX spectrum of typical globular shaped carbide is shown in Fig. 12. The spectrum indicates that these carbides contain a considerable amount of iron and chromium, being identified as $M_{23}C_6$ type. Figure 13 shows the EDX spectrum of the plate shaped precipitates shown in Fig. 11.

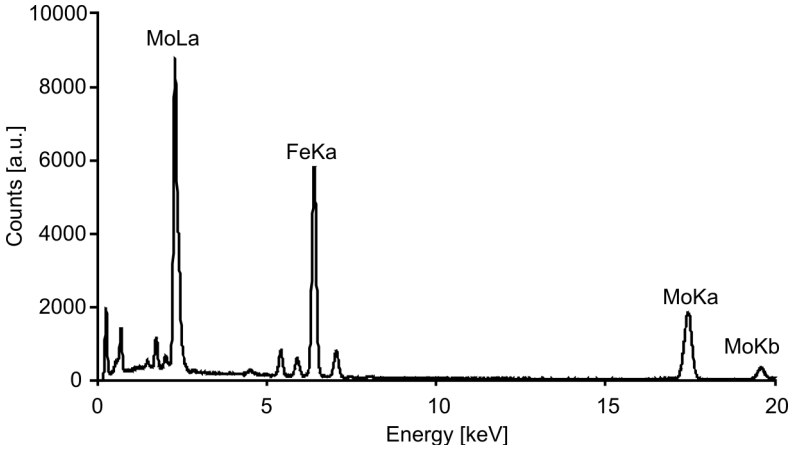

Fig. 13. Typical EDX spectrum of plate shaped carbide rich in molybdenum with a considerable iron content (M_6C type)

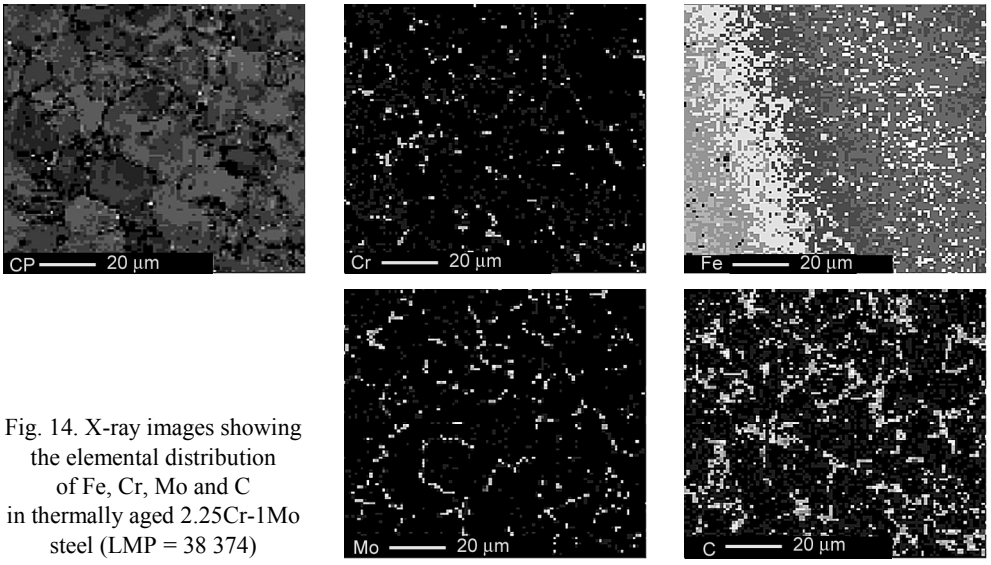

Fig. 14. X-ray images showing the elemental distribution of Fe, Cr, Mo and C in thermally aged 2.25Cr-1Mo steel (LMP = 38 374)

The spectrum indicates that the plate shaped precipitates are molybdenum rich with significant iron content. They are a typical M_6C type of precipitate [7, 10, 11]. Therefore, it is observed that at this stage of ageing, precipitated carbides are a mix-

ture of $M_{23}C_6$ and M_6C type. In this case, the $M_{23}C_6$ type of precipitate contains a greater amount of chromium as compared with the same precipitate having the LMP value 35 402. Observations of other workers [7, 10–12] have also showed that these globular carbides are of $M_{23}C_6$ type, rich in iron and chromium, and that the plate shaped carbides are of M_6C type, rich in molybdenum.

Figure 14 shows X-ray images of a specimen thermally aged at 973 K for 80 h, corresponding to the LMP value of 38 374. Precipitation of chromium and molybdenum carbides at grain boundaries is clearly evident in these figures. Thus, these micrographs very clearly show that as the exposure temperature or time is increased, molybdenum and chromium carbides get precipitated in the sequence of M_3C, M_7C_3, $M_{23}C_6$ and M_6C at the grain boundaries and within the grains themselves. Precipitates also get coarser as we increase the values of the L–M parameters.

3.2. Hardness degradation

The hardness values of both phases, i.e. bainite and ferrite in function of the Larson–Miller parameters are shown in Fig. 15 for both annealed (virgin) material (1223 K for 2 h) and thermally aged specimens. Degradation in hardness of bainitic phase is much stronger (62%) as compared with ferritic phase (12%).

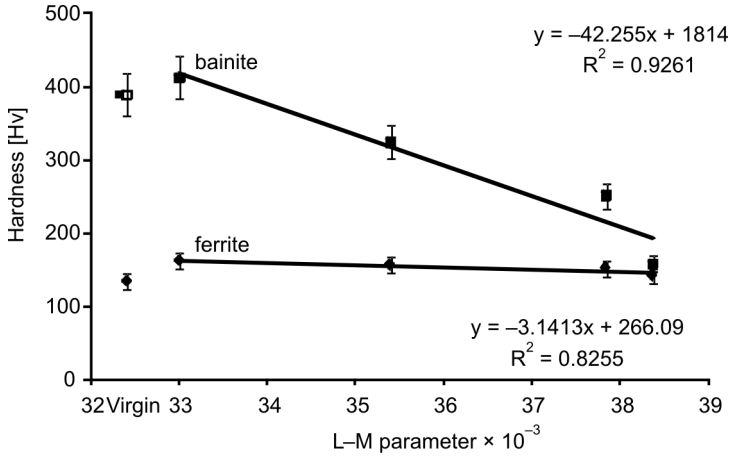

Fig. 15. Dependences of hardness variation of Virgin and thermally aged 2.25Cr-1Mo steel on the L–M parameter

Table 1 gives the hardness values for annealed and thermally aged specimens corresponding to various values of LMP. Hardness has been found to be a sensitive material degradation parameter, sufficient to predict the remaining life of components operating at higher temperatures. It has been reported [13, 14] that in low alloy ferritic steel, solute depletion and precipitate coarsening are the two predominant modes of material degradation during high temperature exposure.

Table 1. Hardness values of samples of annealed and thermally aged 2.25Cr-1Mo steel

Microstructural conditions	Bainite hardness [HV]	Ferrite hardness [HV]
Annealed (1223 K/2 hr)	397	138
Thermally aged (LMP 33.012)	412	162
Thermally aged (LMP 35.402)	324	156
Thermally aged (LMP 37.846)	251	152
Thermally aged (LMP 38.374)	157	141

Results on hardness measurements of samples of thermally aged 2.25Cr-1Mo steel indicate that solute depletion plays a minimum role in the degradation of hardness of this material. This is because the hardness degradation in the ferrite matrix is found to be only up to ca. 12.0%. This could be either because the amounts of solute atoms are very small or their diffusion with time and temperature is very fast. Hardness degradation of up to about 62.0% has been observed in the bainitic phase (Fig. 15). Microstructural examination of this steel at various degrees of ageing indicated a coarsening of carbide particles (Figs. 5, 8, 10 and 11) and a gradual change of their shapes and morphologies. All these observations, therefore, indicate that the predominant modes of hardness degradation in 2.25Cr-1Mo steel are due to a coarsening of alloy carbide precipitates, and a change in their shapes and morphologies. These phenomena are more predominant in bainitic phase, resulting in increased extent of hardness decline of this phase as compared with ferritic phase.

In addition, the variation of the hardness (of both the phases) could be applied to assess the life expectancy of components made out of this material, because the degradation of thermally aged specimens is expected to share similar features with the degradation profile of materials exposed to high temperatures under normal operating conditions. By measuring the hardness of any phase (preferably bainite) after certain, known, number of hours of service, one can ascertain the temperature at which the tube is actually operating. Then, by using the stress rupture plot of this steel, the remaining life of the tube can be estimated [8, 9] and preventive measures could then be taken to avoid potentially catastrophic component failures.

4. Conclusions

The present investigation indicated that in 2.25Cr-1Mo steel, as the ageing temperature or time is increased, molybdenum and chromium carbides get precipitated in the sequence of M_3C, M_7C_3, $M_{23}C_6$ and M_6C at the grain boundaries and within the grains. Precipitation of chromium and molybdenum carbides and coarsening of carbide precipitates are the main contributors of microstructural deterioration in this steel, as a result of increase in the severity of thermal ageing.

The hardness of the both phases (i.e., bainite and ferrite) degrades in function of the L–M parameters, and the hardness degradation of bainite is greater than that of the ferrite phase.

It has been observed that the coarsening of alloy carbide precipitates and the change in their shapes and morphologies are the two predominant factors influencing degradation of hardness in this variety of steel when exposed to service temperatures. Degradation of hardness in function of LMP could be used as a tool for predicting the lifetime of components made up of this steel and operating at higher temperatures.

References

[1] SANDERSON J., [In:] *Ferritic steels for high temperature applications*, Proc. Conf. ASM, A. Khare (Ed.), (1983), p. 178.
[2] PATTERSON S.R., KUNTZ T.A., MOSER R.S., VAILLANCOURT H., [In:] *Boiler tube failure metallurgical guide*, Vol. 1, Techn. Rep.(TR-102433), Electric Power Research Institute, Palo Alto, CA, (1993), p. 26.
[3] VISWANATHAN R., *Damage mechanisms and life assessment of high temperature components*, ASM Int., Metal Park, Ohio, (1989), p. 205.
[4] PATRIARCA D., [In:] *Topical conference on ferritic steels for use in nuclear technologies*, Metall. Soc. AMIE, J.W. Davies, D.J. Michel (Eds.), (1984), p. 107.
[5] THOMSON R.C., Bhadeshia H.K.D.H., Mater. Sci. Tech., 10 (1994), 193.
[6] GOPE N., MUKHERJEE T., SARMA D.S., Mater. Trans. JIM, 33 (1992), 110.
[7] SAROJA S., PARAMESWARAN P., VIJAYALAXMI M., RAGHUNATHAN V.S., Acta Metall. Mater., 43 (1995), 2985.
[8] VISWANATHAN R., PATTERSON S.R., GRUNLOH H., GEHL S., J. Press. Vessel Techn., 116 (1994), 1.
[9] CANE B.J., APLINE P.F., BREAR J.M., J. Press. Vessel Techn., 107 (1985), 295.
[10] JAYAN V., MANDAL P.K., HIRANI M., SANYAL S.K., Mater. Sci. Techn., 15 (1999), 1308.
[11] GANESAN V., RODRIGUEZ P., [In:] *Materials aging and life management*, B. Raj [Ed.], Proc. Int. Symp. Materials Ageing and Life Management, Kalpakkam, India, Allied Publishers Ltd., Chennai, (2000), p. 293.
[12] JAYAN V., KHAN M.Y., HUSAIN M., Mater. Lett., 58 (2004), 2569.
[13] FUJIAMA K., KIMURA K., MURAMATSU M., YAMADA M., ISIJ Int., 30 (1990), 869.
[14] GOPE N., CHATTERJEE A., MUKHERJEE T., SARMA D.S., Metall. Trans. A, 24 (1993), 315.

Received 20 March 2009
Revised 23 April 2009